The 2001 Skyros, Northern Aegean, Greece, earthquake sequence: off - fault aftershocks, tectonic implications, and seismicity triggering

V. G. Karakostas, E. E. Papadimitriou, G. F. Karakaisis, C. B. Papazachos, E. M. Scordilis, G. Vargemezis, and E. Aidona

Geophysics Department, University of Thessaloniki, Thessaloniki, Greece

Received 4 July 2002; revised 29 September 2002; accepted 3 October 2002; published 8 January 2003.

[1] The M_w = 6.4 July 26, 2001 Skyros (North Aegean, Greece) earthquake struck the submarine western end of Northern Aegean Sea causing damage in the nearby Skyros Island. It occurred on a left-lateral NW-SE trending strike slip fault, oriented transverse to the dominant dextral strike-slip faults that are present in the area, appearing to mark the boundary between them and the E-W trending normal faults of the Greek mainland. Foreshock activity started 5 days before the mainshock, and intense aftershock activity followed on the main rupture plane and off fault. The seismogenic structure consists of three clusters with different orientation, independent from the known normal and dextral strike-slip faults. Theoretical static stress changes from the main shock suggests off-fault aftershock triggering, providing a tool for assessing the seismic hazard ensuing from strong aftershocks far from the main rupture. *INDEX TERMS:* 7209 Seismology: Earthquake dynamics and mechanics; 7223 Seismology: Seismic hazard assessment and prediction; 7230 Seismology: Seismicity and seismotectonics. **Citation:** Karakostas, V. G., E. E. Papadimitriou, G. F. Karakaisis, C. B. Papazachos, E. M. Scordilis, G. Vargemezis, and E. Aidona, The 2001 Skyros, Northern Aegean, Greece, earthquake sequence: off - fault aftershocks, tectonic implications, and seismicity triggering, *Geophys. Res. Lett.*, *30*(1), 1012, doi:10.1029/2002GL015814, 2003.

1. Introduction

[2] An M_w = 6.4 earthquake occurred on July 26, 2001 (00:21 UTC) in Northern Aegean, between Skyros and Alonnisos islands.

[3] The seismic activity in Northern Aegean is the consequence of the westward motion of Anatolia, translated into the Aegean microplate along the North Aegean trough and the parallel dextral strike-slip faults, and the north-south expansion of the Aegean itself. The highest activity is concentrated along the northern Aegean trough, which is the most spectacular morphotectonic feature of the area (Figure 1). Right lateral strike-slip faulting prevails, while normal faulting is also present [*Papazachos et al.*, 1998], in agreement with the kinematics of the broader area derived by seismological and geodetic observations [*Papazachos*, 1999; *McClusky et al.*, 2000]. Near the epicentral area four main sequences have occurred in the past forty years (Figure 1), to the northwest (1965 M = 6.1), to the northeast (1967 M = 6.6 and 1968 M = 7.5) and to the southeast (1981 M = 7.2 and M = 6.5). The epicentral area was identified as a possible site for the occurrence of a strong event by *Papadimitriou and Sykes* [2001] who applied an evolutionary stress model in the Northern Aegean area.

[4] The paper analyzes the details of the earthquakes in the Skyros sequence, aiming to contribute to the understanding of the seismotectonic properties in this area where the western termination of the north Aegean strike slip faulting against the mainland of Greece takes place. The co-seismic stress changes associated with the main shock are computed and the areas of static stress increases are correlated with the aftershock spatial distribution.

2. Aftershock Distribution

[5] The recordings of the seismological stations of the national permanent seismological network were adequate to accurately determine the focal parameters of the Skyros sequence earthquakes. The seismological station located at Alonnisos Island (39.170°N – 23.880°E) is the closest one at a distance of about 30 km from the main shock epicenter, contributing significantly in the accurate estimation of focal parameters and especially of the focal depths. All the earthquakes occurring between July 21–August 19, 2001 were analyzed and the P- and S- arrival times were used to compute a mean regional velocity structure, which found to be the same with the regional crustal model suggested by *Panagiotopoulos* [1984], and therefore this later model was adopted in the current work (v_g = 6 km*sec^{-1}, d_g = 19 km, v_b = 6.6 km*sec^{-1}, d_b = 12 km, v_n = 7.9 km*sec^{-1}, d_n = ∞). Repetitive iterations were performed to estimate the mean residuals for each seismological station, until obtaining values that were not changed more than 0.1 sec, and were adopted as station corrections.

[6] The epicentral distribution of the 270 best located events, with vertical (ERZ) and horizontal (ERH) uncertainties in the hypocenters less than 3 km and root-mean-square residual (rms) of 0.30s in most of the cases, delineates a NW-SE trending seismic band, as well as a NE-SW one (Figure 2). Most of the aftershocks are distributed along the NW-SE cluster, which is in agreement with the strike of one of the main shock nodal planes, according to the CMT solution determined by Harvard (strike = 148°, dip = 71°, slip = −1°) and for this reason this is considered as the fault plane, in accordance with the results from inversion of the amplitude spectra of complete waveforms (strike = 150°, dip = 70°, slip = 10° [*Zahradnik*, 2002]). A cluster of 27 small magnitude events (2.2 < M < 4.1) forms a seismic zone west-southwest of the main shock epicenter, oriented NE-SW.

0094-8276/03/2002GL015814$05.00

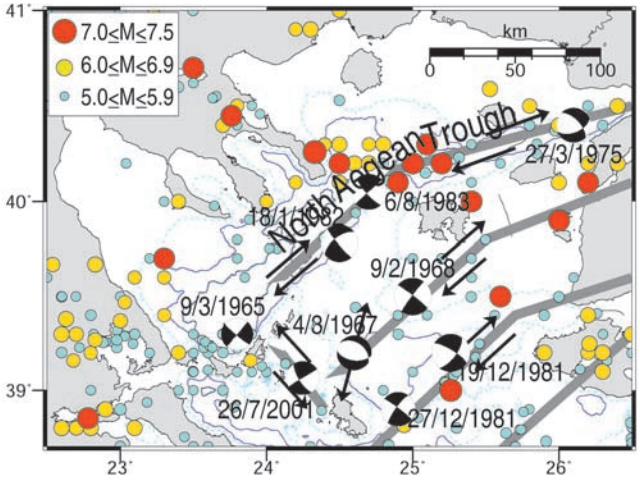

Figure 1. Study area with bathymetry, seismicity ($M \geq 5.0$) and fault plane solutions of earthquakes with $M_w > 6.1$ (1965–2001), exact times are indicated. Lines and arrows indicate the inferred major fault segments and the local motion, respectively.

[7] At least 6 immediate foreshocks of M3.5–5.1 occurred during the five days preceding the main shock (squares in Figure 2) forming a tight spatial cluster at and mostly north of the mainshock epicenter and within 5.0 km. Intense aftershock activity followed the main shock, with four earthquakes of $M > 5.0$ as of July 30, 2001. The 38 km length of the NW-SE trending seismic zone is considerably larger than the fault length corresponding to an M6.4 earthquake (24 km according to *Papazachos* [1989]). Figure 2 shows a change in the strike of the epicentral zone, from 150° to 120°, observed north of the main shock, at the point where the western cluster abuts the main rupture. The extent of the aftershock zone from the mainshock up to its southeastern edge, striking at 150°, is equal to 23 km, in accordance with a fault length capable to produce an M6.4 earthquake. The resulted damage was severe in Skyros Island and negligible in Alonnisos Island, both being at an almost equal distance from the main shock epicenter, suggesting that the rupture was unilateral, starting from the mainshock and propagating southeasterly. Finite-extent waveform modeling evidences that the rupture propagated predominantly unilateral on a 150°-striking fault from NW to SE [*Zahradnik*, 2002].

[8] Vertical sections 15 km wide were computed for the main rupture and the north cluster (119 events with $2.5 < M < 5.3$), trending perpendicular to their mean strike. In section 1 (Figure 3) crossing the north cluster the hypocenters define a zone moderately dipping SW (~55°–60° from 5 km to about 20 km depth). In the next sections that cross the main rupture, a steeply dipping plane is observed (possibly with a dip of ~70° to SW). The largest foreshock has a focal depth greater than the one of the main shock (section 2), an indication that the seismic activity started at the lower part and propagated to the shallower part of the seismogenic layer with the main shock occurrence. In section 2 in addition to the main rupture plane, the foci that belong to the western cluster are shown.

3. Coseismic Coulomb Stress Changes and Triggering of Aftershock Activity

[9] The aftershock distribution suggests that the seismic fault of the main shock is well-approximated with a planar fault, while two other conjugate faults were activated during the seismic excitation. Hence, it is expected that the main shock affected the off-fault aftershock activity, as it has been noticed in several connatural cases [*Stein et al.*, 1994; *Harris*, 1998; *Stein*, 1999]. Stress changes, i.e., values of ΔCFF (changes in Coulomb Failure Function), caused by the mainshock are computed for a sinistral strike-slip fault, according to the NW off-fault aftershock distribution (strike = 140°, dip = 70°, rake = −10°). The stress calculations are performed for an isotropic elastic half space [*Erikson*, 1986; *Okada*, 1992]. The closeness to failure is quantified using the change in Coulomb Failure Function:

$$\Delta CFF = \Delta\tau + \mu(\Delta\sigma + \Delta p) \quad (1)$$

where $\Delta\tau$ is the shear stress change (computed on the slip direction), $\Delta\sigma$ is the fault-normal stress change (positive for extension), Δp is the pore pressure change within the fault, and μ is the friction coefficient which ranges between 0.6 and 0.8 for most rocks [*Harris*, 1998 and references therein]. The pore pressure change resulting from a change in stress under undrained conditions is given by [*Rice and Cleary*, 1976]:

$$\Delta p = -B\frac{\Delta\sigma_{kk}}{3} \quad (2)$$

where B is the Skempton's coefficient. We assume $B = 0.85$ and $\mu = 0.6$ [*Byerlee*, 1978; *Harris*, 1998]. The off-fault aftershocks were triggered in the lobes that are close to the

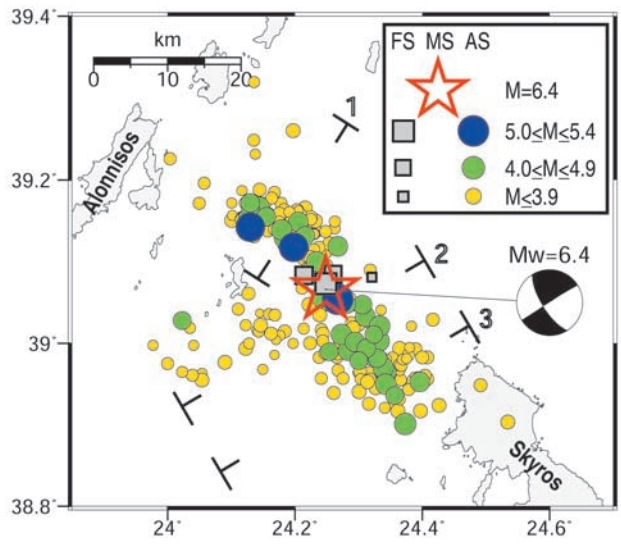

Figure 2. Map of the 2001 Skyros mainshock (big star), foreshocks (squares) and best located aftershocks (circles). The fault plane solution of the main shock is plotted as lower-hemisphere equal-area projection.

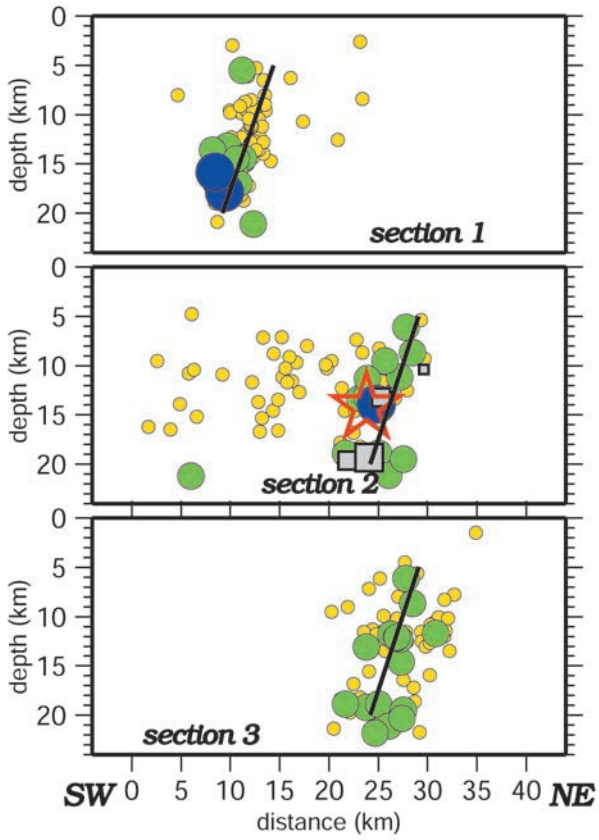

Figure 3. Cross-sections perpendicular to the trend of the zone delineated by the spatial distribution of the events of the sequence (symbols are the same as in Figure 2).

point of rupture initiation (Figure 4a), an observation suggesting that areas of positive stress changes near the focus in a unilateral rupture can be more easily triggered than the areas close to the rupture termination. A late aftershock of M_w5.4 occurred in a positive stress changes area on September 5, 2002 (Figure 4a).

[10] We computed ΔCFF for a sinistral observation plane with strikes ranging between 120° and 160° (Figure 4b), dips ranging between 50° and 90° (Figure 4c) and rakes ranging between 0° and −30° (Figure 4d). Contours represent the 0.1 bar static stress changes, the black one representing the suggested value in the present study. A clockwise shift of the lobes is observed as the strike increases in value, without any remarkable change as far as the dip and rake change concerns. Computations were repeated for the values of friction coefficient ranging between 0.2 and 0.9 (Figure 4e), for Skempton's coefficient ranging between 0.5 and 0.9 (Figure 4f) and observational depth ranging between 8 and 15 km (Figure 4g), evidencing that our results are insensitive to these variations. Maps of ΔCFF for fault plane strike ranging between 138° and 158° (Figure 4h), dip ranging between 50° and 90° (Figure 4i), and strike ranging between −20° and 20° (Figure 4i), indicate that our final results appear robust.

4. Discussion and Conclusions

[11] The Skyros sequence exhibited the complexity of present-day tectonics in Northern Aegean Sea, mostly dextral strike-slip motion on NE-SW trending faults and in lesser degree normal faulting in E-W trending faults takes place [*Papazachos et al.*, 1998]. The fault associated with the Skyros main shock, with a NW-SE strike and sinistral strike-slip motion, is placed rectilinear to the dextral strike-

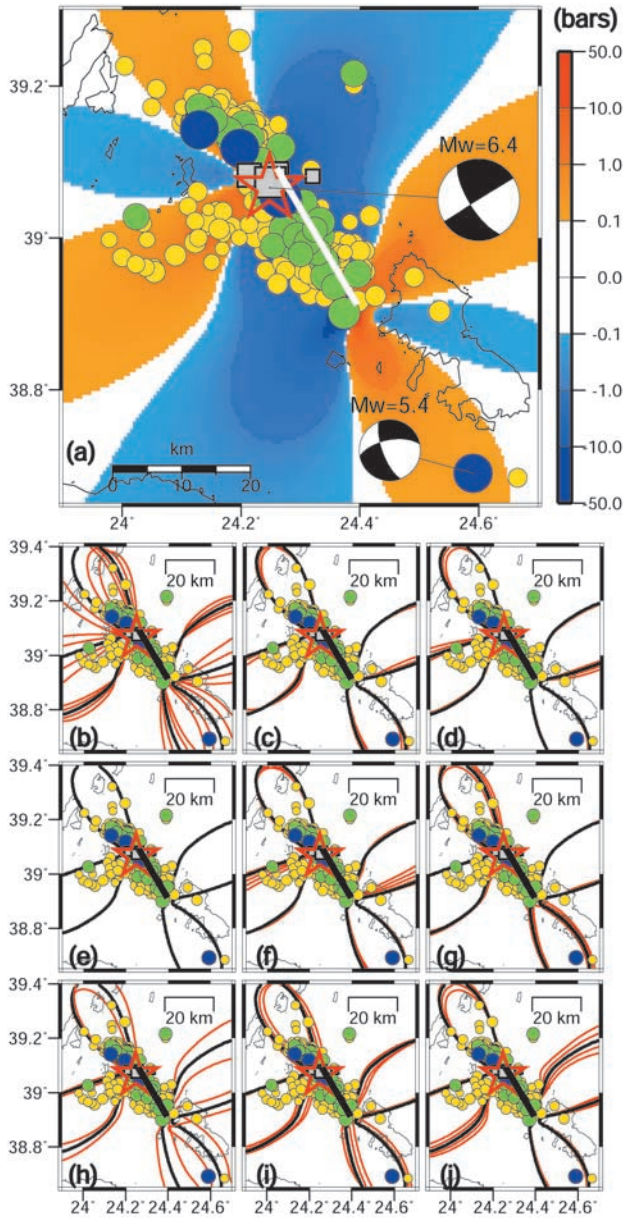

Figure 4. (a) Static Coulomb stress changes (in bars), due to Skyros mainshock, at a depth of 12 km with B = 0.85 and μ = 0.6 for an observational plane with strike = 140°, dip = 70° and rake = −10° and seismicity as in Figure 2. Contours of 0.1 bars are shown for observation plane with strikes ranging between 120° and 160° (b) dips between 50° and 90° (c) and rakes between 0° and −30° (d) Same for values of μ between 0.2 and 0.9 (e) B between 0.5 and 0.9 (f) depths of the observation plane between 8 and 15 km (g) strikes of the fault plane between 138° and 158° (h), dips of the fault plane between 50° and 90° (i), and rakes of the fault plane between −20° and 20° (j).

slip faults, and in particular at a site where the seismicity that runs along these faults seems to cease. Evidence from geomorphology, the distribution of large earthquakes, and geodetic measurements suggests that the active faulting in mainland Greece and the north Aegean Sea is concentrated into a small number of discrete, linear zones that bound relatively rigid blocks [*Goldsworthy et al.*, 2002]. Since the area is submarine and therefore field observations are not available, the present analysis brings more insight on how the transition between the North Aegean parallel NE-SW dextral strike-slip faults and E-W normal faulting of the mainland of Greece takes place. The prevailing N-S extension in the whole back arc Aegean region is then the key motion that results in dextral strike-slip movement on NE-SW trending faults and sinistral strike-slip movement on NW-SE trending faults. This interpretation relies on the assumption that the faults occupying the western Aegean coast are orthogonal to the NE-SW dextral strike-slip faults and mark the boundary between them and E-W normal faults in the mainland of Greece.

[12] The spatial pattern of off-fault aftershock activity is generally well explained in terms of a change in static Coulomb failure stress. The correspondence between seismicity and the positive Coulomb failure stress changes produced by the main shock are in accordance with previous studies that provided a potential explanation of aftershock patterns [e.g, *King et al.*, 1994] and the rate and state-dependent friction model that has successfully explained the decay rate of aftershock sequences [*Dieterich*, 1994; *Gross and Kisslinger*, 1997] and relies on the combination of static stress change from the mainshock and background loading rate to trigger a population of secondary faults. The occurrence of the north cluster could be interpreted as a result of end effects, or as the site of additional fault slip. The western cluster with a northeast orientation is spatially seated almost orthogonal to the strike of the main rupture, in an analogous way of the Big Bear cluster in the case of Landers sequence, which has been attributed to the complex redistribution of stresses caused by the mainshock [*Stein et al.*, 1992; *Harris and Simpson*, 1992; *Hauksson et al.*, 1993]. Although dynamic stress changes found to influence the aftershock occurrence in the propagation direction where static stress changes remained unaffected [*Kilb et al.*, 2002], in the present case off-fault aftershocks appeared to be the result of static stress changes since they occurred in the direction opposite to rupture. Close to a rupture aftershocks could be the result of changes in static stresses, dynamic stresses or both, and therefore, distinguishing between the influence of static and dynamic stresses in earthquake triggering is intriguing, and may help in building a more general understanding of fault interaction [*Marone*, 2000].

[13] The result that aftershocks of the Skyros event may be a product of static stress transfer together with other examples (e.g, Landers-Big Bear sequence) suggests that the seismic hazard posed by aftershocks off the main fault can be assessed by stress-transfer calculations. Aftershocks struck in regions brought from 0.1 to more than 1 bar closer to failure, and the time lag between mainshock and larger aftershocks was short, from some minutes to a few days. Thus, shortly after the main shock occurrence a short-term hazard assessment is feasible regarding triggered aftershocks that may occur closer to urban areas than the main shock.

[14] **Acknowledgments.** This work was greatly improved from the constructive comments by Ross Stein and Debi Kilb and the editorial assistance of Aldo Zollo. The stress tensors were calculated using a program written by *Erikson* [1986] and the expressions of G. Converse. The GMT system [*Wessel and Smith*, 1995] was used to plot the figures. This work was partially supported by the project of the Gen. Secr. Res. & Techn. (Greece) EPAN-M.4.3.6.1/2013555. Department of Geophysics Contribution 607.

References

Byerlee, J. D., Friction of rocks, *Pure Appl. Geophys.*, *116*, 615–626, 1978.

Dieterich, J., A constitutive law for rate of earthquake production and its application to earthquake clustering, *J. Geophys. Res.*, *99*, 2601–2618, 1994.

Erikson, L., User's manual for DIS3D: A three-dimensional dislocation program with applications to faulting in the Earth. *Masters Thesis*, Stanford Univ., Stanford, Calif., 167 pp., 1986.

Goldsworthy, M., J. Jackson, and J. Haines, The continuity of active fault systems in Greece, *Geophys. J. Int.*, *148*, 596–618, 2002.

Gross, S., and C. Kisslinger, Estimating tectonic stress rate and state with Landers aftershocks, *J. Geophys. Res.*, *103*, 7603–7612, 1997.

Harris, R., Introduction to special section: Stress triggers, stress shadows, and implications for seismic hazard, *J. Geophys. Res.*, *103*, 24,347–24,358, 1998.

Harris, R. A., and R. W. Simpson, Changes in static stress on southern California faults after the 1992 Landers earthquake, *Nature*, *360*, 251–254, 1992.

Hauksson, E., L. M. Jones, K. Hutton, and D. Eberhart-Philips, The 1992 Landers earthquake sequence: Seismological observations, *J. Geophys. Res.*, *98*, 19,835–19,858, 1993.

Kilb, D., J. Geomberg, and P. Bodin, Aftershock triggering by complete Coulomb stress changes, *J. Geophys. Res.*, *107*(B4), 2002.

King, G. C. P., R. S. Stein, and J. Lin, Static stress changes and the triggering of earthquakes, *Bull. Seism. Soc. Am.*, *84*, 935–953, 1994.

Marone, C., Shaking faults loose, *Nature*, *408*, 533–534, 2000.

McClusky, S., et al., GPS constraints on crustal movements and deformations in the Eastern Mediterranean (1988–1997): Implications for plate dynamics, *J. Geophys. Res.*, *105*, 5695–5719, 2000.

Okada, Y., Internal deformation due to shear and tensile faults in a half-space, *Bul. Seismol. Soc. Am.*, *82*, 1018–1040, 1992.

Panagiotopoulos, D. G., Travel time curves and crustal structure in the southern Balkan region, *Ph. D. Thesis*, *Univ. of Thessaloniki*, pp. 173 (in Greek), 1984.

Papadimitriou, E. E., and L. R. Sykes, Evolution of the stress field in the Northern Aegean Sea (Greece), *Geophys. J. Intern.*, *146*, 747–759, 2001.

Papazachos, B. C., Measures of earthquake size in Greece and surrounding areas, *Proc. of the 1st Scient. Conf. of Geophysics, Geophys. Soc. of Greece, April 19–21, 1989*, 438–447, 1989.

Papazachos, B. C., E. E. Papadimitriou, A. A. Kiratzi, C. B. Papazachos, and E. K. Louvari, Fault plane solutions in the Aegean and the surrounding area and their tectonic implications, *Boll. Geof. Teor. Appl.*, *39*, 199–218, 1998.

Papazachos, C. B., Seismological and GPS evidence for the Aegean-Anatolia interaction, *Geophys. Res. Lett.*, *26*, 2653–2656, 1999.

Rice, J. R., and M. P. Cleary, Some basic stress diffusion solutions for fluid-saturated elastic porous media with compressible constituents, *Rev. Geophys.*, *14*, 227–241, 1976.

Stein, R. S., The role of stress transfer in earthquake occurrence, *Nature*, *402*, 605–609, 1999.

Stein, R. S., G. C. P. King, and J. Lin, Change in failure stress on the San Andreas and surrounding faults caused by the 1992 M = 7.4 Landers earthquake, *Science*, *258*, 1328–1332, 1992.

Stein, R. S., G. C. P. King, and J. Lin, Stress triggering of the 1994 M = 6.7 Northridge, California, earthquake by its predecessors, *Science*, *265*, 1432–1435, 1994.

Wessel, P., and W. H. F. Smith, New version of the Generic Mapping Tools released, *EOS, Trans. Am. Geophys. U.*, *76*, 329, 1995.

Zahradnik, J., The weak-motion modeling the Skyros island, Aegean Sea, M_w = 6.5 earthquake of July 26, 2001, *Studia Geophysica et Geodaetica*, in press, 2002.

V. G. Karakostas, E. E. Papadimitriou, G. F. Karakaisis, C. B. Papazachos, E. M. Scordilis, G. Vargemezis, and E. Aidona, Geophysics Department, University of Thessaloniki, GR54124, Thessaloniki, Greece.